Journal of Biomechanics 60 (2017) 188–196

Contents lists available at ScienceDirect

Journal of Biomechanics

journal homepage: www.elsevier.com/locate/jbiomech
www.JBiomech.com

Influence of overlapping pattern of multiple overlapping uncovered stents on the local mechanical environment: A patient-specific parameter study

Shuo Wang[a], Yongxue Zhang[b,a], Jiaxuan Feng[b], Yuan Huang[a], Aziz Tokgoz[c], Umar Sadat[d,e], Jonathan H. Gillard[a], Qingsheng Lu[b,1], Zhongzhao Teng[a,c,*]

[a] *Department of Radiology, University of Cambridge, UK*
[b] *Division of Vascular Surgery, Changhai Hospital, Shanghai, China*
[c] *Department of Engineering, University of Cambridge, UK*
[d] *Cambridge Vascular Unit, Addenbrooke's Hospital, Cambridge, UK*
[e] *University Department of Surgery, University of Cambridge, UK*

ARTICLE INFO

Article history:
Accepted 25 June 2017

Keywords:
Aneurysm
Branch
Uncovered stent
Flow
Stress

ABSTRACT

Background: Multiple overlapping uncovered stents (MOUS) system has shown potentials in managing complex aortic aneurysms with side branches involvement. It promotes the development of thrombus by modulating local flow pattern that reduces the wall tension, while maintaining patency of side branches. However the modulation of local hemodynamic parameters depends on various factors that have not been assessed comprehensively.

Methods: Aneurysm 3D geometry was reconstructed based on CT images. One-way fluid-structure interaction analysis was performed to quantify structural stress concentration in the wall, and changes of blood velocity, wall shear stress (WSS), oscillatory shear index (OSI), relative residence time (RRT) and pressure in the sac due to the stent deployment.

Results: High structural stress concentration due to stent deployment was found in the landing zone and it increased linearly with the number of stents deployed. The wall tension in the sac was unaffected by the stent deployment. Stress within the wall was insensitive to the different overlapping pattern. After one stent was deployed, the mean flow velocity in the sac reduced by 36.4%. The deployment of the 2nd stent further reduced the mean sac velocity by 10%. WSS decreased while both OSI and RRT increased after stent deployment, however pressure in the sac remained nearly unchanged. Except for the cases with complete stents struts alignment, different overlapping pattern had little effect on flow parameters.

Conclusions: Mechanical parameters modulated by the MOUS are insensitive to different overlapping pattern suggesting that endovascular procedure can be performed with less attention to the overlapping pattern.

1. Introduction

Flow diverter has been designed to induce thrombosis within intracranial aneurysm by altering blood flow (D'Urso et al., 2011; Mut et al., 2015; Ouared et al., 2016). The underlying mechanism is thought to be related to the formation of mural thrombus, increasing the effective wall thickness and decreasing the lumen radius. This reduces the aneurysm wall tension resulting in a lower risk of wall rupture (Y. Zhang et al., 2014). The primary aim of such a diverter is to treat intracranial lesions that are not effectively managed by traditional approaches, including coil embolization, conventional high porosity stents and coils, parent artery occlusion and neurosurgical procedures, e.g., aneurysm clipping, resection and bypass. Further technique developments have improved the cure rate with low complication rate. This technique has transformed the management of intracranial aneurysms and become a preferred treatment option for large or giant wide-necked lesions (Walcott et al., 2016).

The attractive advantages of this technology exist in its minimally invasive nature and the capacity to keep long-term

---

* Corresponding author at: Department of Radiology, University of Cambridge, Box 218, Cambridge Biomedical Campus, Cambridge CB2 0QQ, UK.

E-mail addresses: luqs@xueguan.net (Q. Lu), zt215@cam.ac.uk (Z. Teng).

[1] Co-corresponding author at: Division of Vascular Surgery, Changhai Hospital, 168 Changhai Road, 200433 Shanghai, China.

http://dx.doi.org/10.1016/j.jbiomech.2017.06.048
0021-9290/© 2017 Elsevier Ltd. All rights reserved.

patency of side branches (Kallmes et al., 2007). Encouraged by the success of flow diverter in treating intracranial aneurysms, researchers have attempted to use a similar strategy to manage complex aortic aneurysms by using multiple overlapping uncovered stents (MOUS). However controversial findings were reported due to the difference in hemodynamic environment and lesion size between intracranial and aortic aneurysm. Aneurysm expansion and rupture after uncovered metal stents deployment (Debing et al., 2014; Lazaris et al., 2012; Sultan et al., 2014) and stent longitudinal shortening have been reported (Sultan and Hynes, 2013), while promising outcomes were also documented (Y. Zhang et al., 2014; Zhang et al., 2013). This implies that there is a need of refined patient selection and further comprehensive studies to identify the key factors affecting the outcome of MOUS.

This study is designed to quantify the MOUS deployment induced changes of local hemodynamic environment, including the flow velocity and rate in the sac and side branches, wall shear stress (WSS), oscillatory shear index (OSI), relative residence time (RRT) and pressure in the sac and structural stress in the landing zone, by performing parameter analyses. The obtained results will help understand the mechanism of failure and success in different patient cohort, key factors affecting these hemodynamic parameters, as well as how the system should be further optimised.

2. Materials and methods

2.1. The patient

The patient involved in the analysis is from the cohort reported previously (Y. Zhang et al., 2014; Zhang et al., 2013). This study was approved by the review board of Changhai Hospital, Shanghai, China. The patient was a 68-year old male with a complex thoracic aortic aneurysm (maximum diameter was 70.1 mm) (Fig. 1). Medical history included pulmonary function impairment, grade II hypertension (146/92 mmHg; heart rate of 80/min) and coronary artery disease that had been previously treated by stenting. Given his multiple comorbidities and the risk of spinal cord ischemia after stent-grafting (at the level of T11-L1), the patient was judged unfit for either open surgery or traditional endovascular aortic repair by the multidisciplinary surgical team consisting of vascular surgeons, cardio-thoracic surgeons, and anesthetists. The MOUS strategy was therefore explained to the patient, who gave a written informed consent for the procedure. Closed-cell, self-expandable and uncovered sinus-XL stents from OptiMed (Ettlingen, Germany) were used (Fig. 1D).

2.2. Patient-specific 3D aneurysm geometry reconstruction

Segmentation was performed based on pre-operative contrast-enhanced computed tomography angiography (CTA) images to identify aortic wall, calcium and thrombus using an in-house program developed in MATLAB R2016a (The MathWorks, Inc., USA). Surrounding tissues and organs, e.g., spine and liver, were not considered. In this study, the CTA resolution was $0.683 \times 0.683 \times 0.8$ mm^3, the aortic wall thickness was about 2.5 mm and the diameters of visible sub-branches ranged from 2.9 mm to 6.0 mm and the wall thickness of sub-branches was about 1.0 mm.

To reduce the effect of smoothing operation during the 3D geometry reconstruction, CTA images were resampled with a voxel size of $0.1 \times 0.1 \times 0.1$ mm^3. The model reconstruction included the aorta reconstruction and sub-branches reconstruction. Firstly, the resampled CTA images were imported into an in-house MATLAB platform to semi-automatically segment aortic lumen, calcium, thrombus and aortic wall by trained operators (Huang et al., 2016). The segmented contour information was translated to a voxel-based label map in 3D Slicer (http://www.slicer.org). The lumens of sub-branches were segmented using threshold algorithm and a uniform wall thickness of 1 mm for all sub-branches was applied by dilating the lumen label map. The voxel-based label maps of aortic components and sub-branches were then merged and smoothed using Gaussian Filter. After completion of the final voxel-based label maps, the surface of each object were generated using fast marching method in 3D Slicer and imported to VMTK (http://www.vmtk.org/) and smoothed using Taubin's algorithm (Fig. 1C) (Taubin, 1995). Finally, surfaces of inlet and outlet of AAA and the outlet of each sub-branch were clipped and extended 15 times of the local diameter to eliminate inlet and outlet effect. The 3D geometry was then generated using these surfaces and adaptive meshing was made in ICEM (ANSYS Inc., USA). For the baseline model (without any stent), 409,357 tetrahedron elements were generated for the solid part and 80,562 tetrahedral elements and 175,691 prism elements for the fluid part.

2.3. 3D reconstruction of uncovered stents

The geometry of the bare metal stent was reconstructed according to parameters provided by the supplier in Creo2.0 (PTC, Needham, USA) (Fig. 1D) and exported to ICEM for meshing. A single stent was meshed with 119,592 hexahedron elements.

2.4. Finite element analysis

In this study, a one-way fluid-structure interaction (FSI) analysis was performed to re-predict mechanical conditions before and after stent deployment to assess the influence of stent deployment on critical mechanical conditions within the aneurysmal structure and blood flow in the sac and side branches. Detailed processes for the cases with stents deployment can be found in the flowchart shown in Fig. 2.

2.4.1. Virtual stent deployment

Since CTA images were acquired under pressurised condition, an inverse procedure with a pressure level of 110 mmHg (patient's mean blood pressure) and axial stretch 2.5% at both ends was followed to obtain the computational starting shape (Raghavan et al., 2006). Stent was assumed to be a linear material with Young's modulus and Poison's ratio of 75 GPa and 0.333, respectively. Modified Mooney-Rivlin model was used to describe the material properties of aortic wall, thrombus and calcium,

$$W = C_1(\bar{I}_1 - 3) + D_1[e^{D_2(\bar{I}_1 - 3)} - 1] + \kappa(J - 1)$$

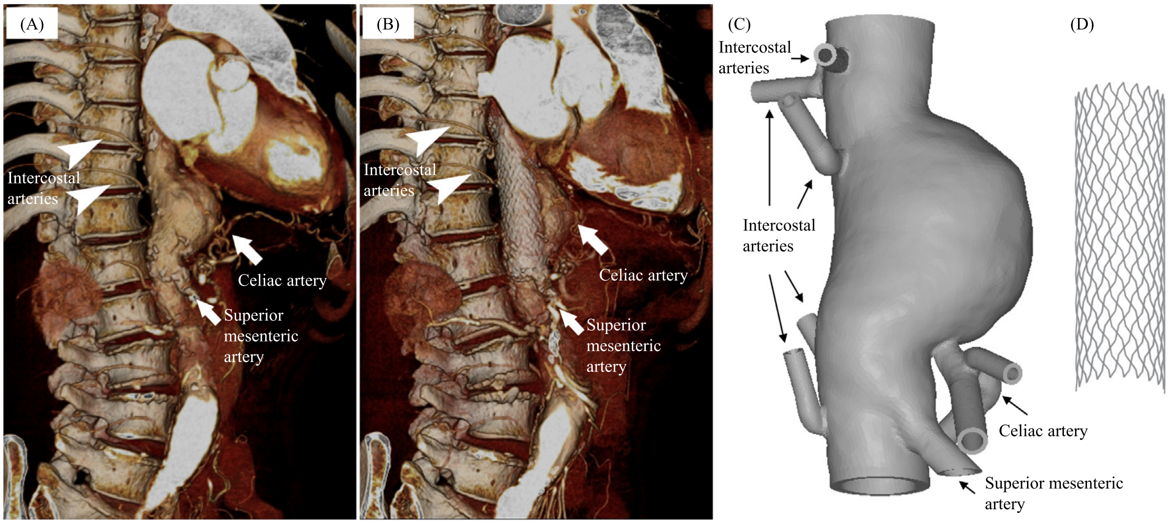

Fig. 1. The configuration of a complex aortic aneurysm with vital branches involvement (side branches were marked with arrow heads and arrows) (A: lesion configuration before stent deployment; B: the configuration at 12 months after 4-layer stents deployment, the aneurysm was partially thrombosed and side branches maintained their patency; C: reconstructed 3D aneurysm geometry; and D: reconstructed 3D stent geometry [only half was shown for a better visualization]).